Inclusion Compounds of Tetrakis(4-nitrophenyl)methane: C−H···O Networks, Pseudopolymorphism, and Structural Transformations

Ram Thaimattam,[†] Feng Xue,[‡] Jagarlapudi A. R. P. Sarma,*[,§] Thomas C. W. Mak,*[,‡] and Gautam R. Desiraju*[,†]

Contribution from the School of Chemistry, University of Hyderabad, Hyderabad 500 046, India, Department of Chemistry, The Chinese University of Hong Kong, Shatin, New Territories, Hong Kong SAR, P. R. China, and Molecular Modeling Group, Organic Division-I, Indian Institute of Chemical Technology, Hyderabad 500 007, India

Received August 25, 2000. Revised Manuscript Received November 28, 2000

Abstract: Tetrakis(4-nitrophenyl)methane is a new host material with considerable structural adaptability over a range of solvents. The crystal structures of 14 of these solvates have been determined and classified into three groups. The diamondoid group, wherein the host molecules form a 2-fold interpenetrated diamondoid network structure, is unprecedented in that network connections are made exclusively with weak C−H···O and $\pi\cdots\pi$ interactions. This group consists of the solvates of THF, dioxane, nitrobenzene, 4-bromoanisole, anisole, phenetole, *p*-xylene, and chlorobenzene. The rhombohedral group, which is characterized by specific host···guest interactions of the C−H···O and halogen···O_2N type, consists of the solvates of $CHCl_3$ and $CHBr_3$ and somewhat surprisingly DMF, which shows an unusual 3-fold disorder mimicking in part the shape and size of the haloform molecules though not their orientation. The third group comprises solvent-rich solvates of the host with mesitylene, collidine, and *o*-xylene with quite different crystal structures. The THF solvate was found to lose solvent over limited temperature ranges transforming reversibly from the diamondoid structure to the rhombohedral structure. A mechanism for this process is outlined. Material from which solvent has been removed by heating was also found to resolvate upon soaking in appropriate solvents. In summary, the title compound forms a host network that is partially robust and in part flexible. It is possible that this fluxional nature of the host network derives from the weakness of the connecting interactions.

Introduction

The crystal chemistry of the tetraphenylmethanes has always offered opportunities for the study of packing preferences and solid-state properties. Kitaigorodskii recognized that molecules of the type Ph_4X (X = C, Si, Ge, Pb, Sn) form an isomorphous series.[1] All adopt tetragonal symmetry (space group $P\bar{4}2_1c$) with the unique axis in the range 6.65−7.26 Å). More recently, Brock and co-workers showed that close packing of phenyl rings via edge-to-face C−H···π interactions leads to the formation of T_d symmetry voids, with the molecules lying on the $\bar{4}$ axis.[2] Independently, Dance and Scudder identified this phenyl packing pattern, the tetraphenyl embrace, as a common one in molecular crystals.[3]

We have previously explored the packing properties of tetrakis(4-bromophenyl)methane), but the additional possibility of Br···Br interactions leads to the formation of supramolecular tetrahedral Br_4 clusters.[4c] This supramolecular synthon may be replaced with the molecular synthon CBr_4 leading to an equivalent structure, namely the 1:1 molecular complex of tetraphenylmethane and CBr_4. Similar topologies and symmetries were observed in tetrakis(4-iodophenyl)methane,[4b] the 1:1 molecular complex of tetraphenylmethane and CCl_4,[4a] and tetrakis(4-ethynylphenyl)methane.[5a] All these structures are of the diamondoid type[5,6] and are interpenetrated.[6b,c,7]

In contrast, it was found that tetrakis(4-nitrophenyl)methane, **1**, forms as many as 14 crystalline solvates when crystallized from various solvates. This paper describes the crystal structures of these solvates and their classification into three groups. Also discussed is the desolvation and resolvation behavior of some

[†] University of Hyderabad.

[‡] The Chinese University of Hong Kong.

[§] Indian Institute of Chemical Technology.

(1) Kitaigorodskii, A. I. *Molecular Crystals and Molecules*; Academic Press: New York, 1973; pp 67−71.

(2) (a) Lloyd, M. A.; Brock, C. P. *Acta Crystallogr.* **1997**, *B53*, 780−786. (b) Brock, C. P.; Dunitz, J. D. *Chem. Mater*. **1994**, *6*, 1118−1127.

(3) Dance, I.; Scudder, M. *Chem. Eur. J*. **1996,** *2*, 481−486.

(4) (a) Anthony, A.; Desiraju, G. R.; Jetti, R. K. R.; Kuduva, S. S.; Madhavi, N. N. L.; Nangia, A.; Thaimattam, R.; Thalladi V. R. *Cryst. Eng.* **1998**, *1*, 1−18. (b) Thaimattam, R.; Reddy, D. S.; Xue, F.; Mak, T. C. W.; Nangia, A.; Desiraju, G. R. *New J. Chem*. **1998**, *22*, 143−148. (c) Reddy, D. S.; Craig, D. C.; Desiraju, G. R. *J. Am. Chem. Soc.* **1996**, *118*, 4090−4093.

(5) Some references that describe organic diamondoid solids: (a) Galloppini, E.; Gilardi, R. *Chem. Commun*. **1999**, 173−174. (b) Wuest, J. D. *Mesomolecules: From Molecules to Materials*; Mendenhall, G. D.; Greenberg, A.; Liebman, J. F., Eds.; Chapman & Hall: New York, 1995; pp 107−131. (c) Wang, X.; Simard, M.; Wuest, J. D. *J. Am. Chem. Soc.* **1994**, *116*, 12119−12120. (d) Wang, X.; Simard, M.; Wuest, J. D. *J. Am. Chem. Soc.* **1991**, *113*, 14696-4698. (e) Ermer, O.; Lindenberg, L. *Helv. Chim. Acta* **1991**, *74*, 825−877. (f) Ermer, O. *J. Am. Chem. Soc.* **1988**, *110*, 3747−3754.

(6) Selected references to inorganic or metal−organic diamondoid solids: (a) Evans, O. R.; Xiong, R.-G.; Wang, Z.; Wong, G. K.; Lin, W. *Angew. Chem., Int. Ed.* **1999**, *38*, 536−538. (b) Batten, S. R.; Robson, R. *Angew. Chem., Int. Ed.* **1998**, *37*, 1460−1494 and the references therein. (c) Blake, A. J.; Champness, N. R.; Chung, S. S. M.; Li, W.-S.; Schröder, M. *Chem. Commun.* **1997**, 1005−1006. (d) Zaworotko, M. J. *Chem. Soc. Rev.* **1994**, *23*, 283−288.

(7) (a) Carlucci, L.; Ciani, G.; Moret, M.; Proserpio, D. M.; Rizzato, S. *Angew. Chem., Int. Ed*. **1999**, *38*, 1506−1510. (b) Hoskins, B. F.; Robson, R. *J. Am. Chem. Soc*. **1990**, *112*, 1546−1554. (c) For an alternative mode of close-packing of large network structures, see: Batten, S. R.; Hoskins, B. F.; Moubaraki, B.; Murray, K. S.; Robson, R. *Chem. Commun*. **2000**, 1095−1096.

10.1021/ja0031826 CCC: $20.00
Published on Web 04/20/2001

Table 1. Crystallographic Data for the Inclusion Compounds of Tetrakis(4-nitrophenyl)methane

	2	**3**	**4**	**5**	**6**	**7**	**8**
empirical formula	$(C_{25}H_{16}N_4O_8)\cdot(C_4H_8O)$	$(C_{25}H_{16}N_4O_8)_3\cdot(C_4H_8O_2)_2$	$(C_{25}H_{16}N_4O_8)_3\cdot(C_6H_5NO_2)_2$	$(C_{25}H_{16}N_4O_8)_2\cdot(C_7H_7OBr)$	$(C_{25}H_{16}N_4O_8)_2\cdot(C_7H_8O)$	$(C_{25}H_{16}N_4O_8)_2\cdot(C_4H_{10}O)$	$(C_{25}H_{16}N_4O_8)_2\cdot(C_8H_{10})$
solvent	THF	dioxane	nitrobenzene	4-bromoanisole	anisole	phenetole	*p*-xylene
formula wt	572.5	1589.4	582.5	1187.9	1109.0	1123.0	1107.0
crystal system	orthorhombic	tetragonal	tetragonal	orthorhombic	orthorhombic	orthorhombic	orthorhombic
space group	*Fddd* (no. 70)	$P4_2/n$ (no. 86)	$P4_2/n$ (no. 86)	*Pbcn* (no. 60)	*Pbcn* (no. 60)	*Pbcn* (no. 60)	*Pbcn* (no. 60)
a (Å)	24.365(3)	13.139(6)	13.055(2)	18.340(2)	18.236(2)	18.257(4)	18.246(4)
b (Å)	28.629(4)	13.139(6)	13.055(2)	15.680(2)	15.685(1)	15.668(3)	15.668(3)
c (Å)	15.257(1)	23.087(13)	22.754(5)	18.216(2)	18.191(1)	18.333(4)	18.237(4)
α (deg)	90	90	90	90	90	90	90
β (deg)	90	90	90	90	90	90	90
γ (deg)	90	90	90	90	90	90	90
Z	16	2	2	4	4	4	4
V (Å^3)	10642.5(9)	3986(3)	3878.1(2)	5238.4(5)	5203.2(5)	5244 2(19)	5213.6(18)
D_{calc} (Mg/m^3)	1.429	1.324	1.496	1.506	1.416	1.422	1.410
R_1	0.0689	0.1463	0.0565	0.0651	0.0792	0.0775	0.0550
wR_2	0.1821	0.4051	0.1046	0.1732	0.1711	0.2171	0.1343
Goof	1.163	1.335	1.047	0.904	1.218	0.990	1.306

	9	**10**	**11**	**12**	**13**	**14**	**15**
empirical formula	$(C_{25}H_{16}N_4O_8)_2\cdot(C_6H_5Cl)$	$(C_{25}H_{16}N_4O_8)_3\cdot(CHCl_3)$	$(C_{25}H_{16}N_4O_8)_3\cdot(CHBr_3)$	$(C_{25}H_{16}N_4O_8)_3\cdot(C_3H_7NO)$	$(C_{25}H_{16}N_4O_8)\cdot(C_9H_{12})_2$	$(C_{25}H_{16}N_4O_8)\cdot(C_8H_{11}N)_2$	$(C_{25}H_{16}N_4O_8)_2\cdot(C_8H_{10})_2$
solvent	chlorobenzene	$CHCl_3$	$CHBr_3$	DMF	mesitylene	collidine	*o*-xylene
formula wt	1113.4	1620.6	1754.0	1574.3	740.8	742.8	1213.2
crystal system	orthorhombic	trigonal	trigonal	trigonal	monoclinic	tetragonal	monoclinic
space group	*Pbcn* (no. 60)	$R\bar{3}$ (no. 148)	$R\bar{3}$ (no. 148)	$R\bar{3}$ (no. 148)	$P\bar{1}$ (no. 2)	$P\bar{4}2_1c$ (no. 114)	*C*2/*c* (no. 15)
a (Å)	18.228(4)	22.276(1)	15.437(2)	15.427(2)	9.968(1)	10.938(1)	18.642(3
b (Å)	15.645(3)	22.276(1)	15.437(2)	15.427(2)	13.147(1)	10.938(1)	18.706(4)
c (Å)	18.205(4)	25.348(1)	15.437(3)	15.427(2)	15.747(1)	15.963(1)	34.164(6)
α (deg)	90	90	93.02(1)	91.73(1)	72.40(1)	90	90
β (deg)	90	90	93.02(1)	91.73(1)	80.83(1)	90	97.36(5)
γ (deg)	90	120	93.02(1)	91.73(1)	88.49(1)	90	90
Z	4	6	2	2	2	2	8
V (Å^3)	5192.9(2)	10893.0(8)	3662.8(4)	3666.4(4)	1941.4(3)	1910.0(2)	11815(6)
D_{calc} (Mg/m^3)	1.423	1.482	1.590	1.426	1.267	1.292	1.364
R_1	0.0605	0.0483	0.0704	0.0696	0.0711	0.0707	0.0759
wR_2	0.1629	0.1331	0.1301	0.0707	0.1981	0.1756	0.2183
Goof	1.153	1.036	1.228	1.173	1.09	0.945	0.919

of the solvates and, finally, the structural relationship between the groups. In short, we present the rich structural chemistry of a novel and highly efficient host material.[8]

Experimental Section

Tetrakis(4-nitrophenyl)methane, **1**, was prepared according to literature procedures.[9] To 40 mL of fresh fuming nitric acid maintained at 0 °C was added tetraphenylmethane (7.4 g, 23 mM) slowly over 15 min. To this mixture was slowly added a mixture of acetic anhydride (12.5 mL) and acetic acid (25 mL) while maintaining the same temperature. Stirring was continued for another 15 min and the reaction mixture was then diluted with acetic acid (50 mL) to precipitate the crude product of **1**, which was filtered and washed with acetic acid (10 mL). Compound **1** was further purified by recrystallization from THF to yield 5.2 g of powder (45%), mp 339 °C; ^{1}H NMR (200 MHz, $CDCl_3$) δ 8.23 (d, $J = 9$ Hz, 4H), 7.42 (d, $J = 9$ Hz, 4H). Interestingly, the ^{1}H NMR spectrum indicated the presence of THF in the material.

Recrystallization Experiments. Diffraction quality crystals of complexes **2**−**9** and **12**−**15** were prepared by crystallizing compound **1** from the respective solvents (Table 1). Crystallization of **1** from either pure $CHCl_3$ or CH_2Cl_2 produced only microcrystalline material. When crystallization was attempted from a mixture of $CHCl_3/CH_2Cl_2$ (1:50), good quality crystals of the chloroform solvate **10** were obtained. Attempts to obtain the $CHBr_3$ solvate by recrystallization from pure $CHBr_3$ were likewise unsuccessful. Once again, however, crystallization from 1:50 $CHBr_3/CH_2Cl_2$ yielded good single crystals of **11**. All attempts to obtain solvent-free crystals of **1** were unsuccessful. As will be seen in the following discussion, the structural adaptability in this system is so great that any solvent used for recrystallization is included easily in the crystal framework.

X-ray Crystallography. Intensities were collected on Rigaku AFC7R and Enraf Nonius MACH3 diffractometers, a Rigaku RAXIS IIC imaging plate, and a Bruker SMART 1000 CCD area detector with Mo Kα radiation ($\lambda = 0.71073$ Å) at 294 K. Empirical absorption corrections were applied to the raw intensities as follows: a pseudoellipsoidal fit to the ψ-scan data[10] from the AFC7R diffractometer, Fourier coefficient fitting of symmetry-equivalent reflections with the ABSCOR program[11] for RAXIS IIC data, and multiscan correction with the SADABS program[12] for data collected on the SMART CCD system. No absorption correction was applied to the intensity data collected on

(8) Some of the recent references on host−guest materials: (a) Toda, F.; Miyamoto, H.; Inoue, M.; Yasaka, S.; Matijasic, I. *J. Org. Chem.* **2000**, *65*, 2728−2732. (b) Weber, E.; Hens, T.; Brehmer, T.; Csöregh, I. *J. Chem. Soc., Perkin Trans. 2* **2000**, 235−241. (c) Jetti, R. K. R.; Xue, F.; Mak, T. C. W.; Nangia, A. *J. Chem. Soc., Perkin Trans. 2* **2000**, 1223−1232. (d) Kobayashi, K.; Shirasaka, T.; Sato, A.; Horn, E.; Furukawa, N. *Angew. Chem., Int. Ed.* **1999**, *38*, 3483−3486. (e) MacGillivray, L. R.; Atwood, J. L. *Angew. Chem., Int. Ed.* **1999**, *38*, 1018−1033. (f) Chui, S. S.-Y.; Lo. S. M.-F.; Charmant, J. P. H.; Orpen, A. G.; Williams, I. D. *Science* **1999**, *283*, 1148−1150. (g) Caira, M. R.; Nassimbeni, L. R.; Toda, F.; Vujovic, D. *J. Chem. Soc., Perkin Trans. 2* **1999**, 2681−2684. (h) Yaghi, O. M.; Li, H.; Davis, C.; Richardson, D.; Groy. T. L. *Acc. Chem. Res.* **1998**, *31*, 474−484. (i) Swift, J. A.; Pivovar, A. M.; Reynolds, A. M.; Ward, M. D. *J. Am. Chem. Soc.* **1998**, *120*, 5887−5894. (j) Endo, K.; Ezuhara, T.; Koyanagi, M.; Masuda, H.; Aoyama, Y. *J. Am. Chem. Soc.* **1997**, *119*, 499−505. (k) Bishop, R. *Chem. Soc. Rev.* **1996**, 311−320. (l) Sharma, C. V. K.; Panneerselvam, K.; Shimoni, L.; Katz, H.; Carrell, H. L.; Desiraju, G. R. *Chem. Mater.* **1994**, *6*, 1282−1292.

(9) Neugebauer, F. A.; Fischer, H.; Bernhardt, R. *Chem. Ber.* **1976**, *109*, 2389−2394.

(10) Sparks, R. A. *Crystallographic Computing Techniques*; Ahmed, F. R., Ed.; Munksgaard: Copenhagen, 1976; p 452.

(11) Hagashi, T. *ABSCOR*; An Empirical Absorption Correction Based on Fourier Coefficient Fitting; Rigaku Corporation: Tokyo, 1995.

the MACH3 diffractometer. Structure solution was carried out with SHELXS-86 and SHELXS-97 while the refinements were performed with either SHELXL-93 or SHELXL-97 program packages.[13] Details of data collection, structure solution, and refinement are summarized in Table 1. In the case of the disordered structures, the refinement of the site occupancy factors and atomic displacement factors were carried out in stages and in no case were both parameters allowed to vary simultaneously.

Desolvation and Resolvation Experiments. Crystalline **2** (4 mM) was heated at 65, 78, 83, 97, and 110 °C for 2 h under a mild vacuum (20 mmHg). Sufficient care was taken to ensure that material was not lost upon application of vacuum. The weight loss of the sample at these temperatures (except at 65 °C where the loss is minimal) was measured on an electronic balance (Mettler AJ100) at regular intervals. All weight loss was assigned to solvent only. All experiments were repeated with powdered samples and similar weight losses were obtained. The single crystal samples became opaque upon losing solvent. In the resolvation experiments, the samples that were heated at the above temperatures for 2 h were soaked for 3 days at 0 °C in a minimum amount of THF just enough to wet the crystals. Similar procedures were also followed in the solvent exchange experiments. The samples were initially dried on filter paper and then left in open air for ~3 days. The solvent exchange was monitored by ^{1}H NMR and X-ray powder spectra.

Powder X-ray Analysis and Simulations. Powder spectra of some solvated, desolvated, resolvated, and solvent exchanged **2** were recorded on a Siemens 5000 diffractometer with Cu Kα radiation. Quantitative phase analysis was carried out on the X-ray powder spectrum of **2** heated at 97 °C with the Rietveld method in the Cerius^2 program.[14] Two phases, THF solvate **2** and $CHCl_3$ solvate **10**, were considered for the refinements. The cell parameters of solvate **10** were also allowed to vary along with percentage composition (the initial composition taken was 1:1) while the cell parameters of **2** and the atomic and thermal parameters of both phases were fixed. The Rietveld refinement converged to a final R factor of 32.29 ($R - WP = 48.34$, goodness of fit, $S = 1.79$). The two phases **2** and **10** converged to 9.03 and 90.97%, respectively. In another set of Rietveld refinements, the THF-II (rhombohedral phase) was used instead of the $CHCl_3$ solvate **10**. However, neither the percentage compositions nor the cell parameters varied significantly.

Energy Calculations. The nitrobenzene dimer energy was calculated with the Hartree−Fock ab initio method at the 6-31G** level.[15] Due to the constraints involved in considering two molecules of **1** independently, two preoptimized nitrobenzene molecules were taken. The initial energy was calculated based on the dimer geometry as seen in **2**. The geometry was then optimized to produce a highly overlapped inverted dimer. The energy difference between the propeller and V-shaped conformations of **1** was calculated with AM1 methods.[16] The donor strengths of mesitylene and collidine were correlated from the HOMO energies as obtained from AM1 calculations.

The Burchart-DREIDING force field with Gasteiger charges was used for the packing energy calculations (Cerius^2). The Ewald summation method was used. Due to the uncertainties involved in the positions of the guest molecules (owing to disorder), they were optimized with AM1 without varying their relative position and orientation in the unit cell. In **5**−**9**, the guest molecules lie on the 2-fold axis and only one of the possible two orientations was considered. The orientations that arise due to non-2-fold disorder of guests in **5** and **9** were, however, taken into account. Similarly, in **8**, only three H atoms of each methyl group of the guest were included. In **12**, the 3-fold disordered DMF guest molecule was considered in one of the three possible ways while in **15**, only one collidine was considered among the possible four. Packing coefficients of the solvates and desolvates are based on free-volume calculations (Cerius^2) and the results are given in Table 2.

Table 2. Packing Potential Energies (PPE in kcal/mol) and Packing Coefficients (PC) in Solvates **2**−**15**

		PPE			PC	
structure	n	E_a	E_b	E_c	with guest	without guest
2	1	−55.85	−39.55	−16.30	77.4	66.2
3	0.67	−45.49	−37.31	−12.28	76.2	67.8
4	0.67	−55.90	−40.05	−23.67	76.2	65.8
5	0.5	−49.99	−36.23	−26.98	78.4	56.3
6	0.5	−47.90	−36.14	−23.52	76.2	67.6
7	0.5	−48.35	−36.74	−23.21	78.1	67.2
8	0.5	−48.53	−36.33	−24.41	77.5	67.4
9	0.5	−46.10	−35.93	−21.02	77.0	54.6
10	0.33	−44.23	−38.95	−15.86	76.4	71.9
11	0.33	−44.75	−38.98	−17.35	76.5	72.0
12	0.33	−48.32	−39.13	−27.61	77.7	70.3
13	2	−73.13	−24.41	−24.36	74.4	44.9
14	1	−43.59	−18.16	−25.43	77.2	45.0
15	1	−56.78	−28.33	−28.45	75.6	60.4

n = number of guest molecules per molecule of host. E_a is the PPE/molecule of the host for the host−guest system = PPE per unit cell/Z_{host}. E_b is the stabilization in PPE/molecule of the host without solvent molecules (host alone) = PPE$_{(without\ guest)}$/unit cell]/$Z_{(host)}$. E_c is the stabilization in the PPE/molecule of host due to one molecule of the guest = $E_a - E_b/n$.

Results and Discussion

Diamondoid Group. (a) Solvate 2, (1)·(THF). As shown in Figure 1, the stacking of host molecules **1** in **2** lying on 2-fold axes along [001] (space group *Fddd*) resembles the tetraphenyl embrace of Dance, but the arrangement does not involve edge-to-face phenyl−phenyl interactions. The separation of the central C-atoms is at a distance of ~7.7 Å as observed in other tetraphenylmethanes.[1] Of the 16 tetraphenylmethanes in the CSD (October 1999 release, Version 5.18),[17] 14 have the propeller conformation and only two are V-shaped. Indeed, in compound **1** the propeller conformation is more stable than the V-shaped one by around 4.5 kcal/mol (MOPAC, AM1), and this is in agreement with the CSD statistics. Yet it is not the observed conformation in solvate **2**, or for that matter in any of the other solvates in this study: all of them have the V-shaped conformation. Now, the propeller conformation, which is already the more stable one, is further stabilized in crystal structures of tetraphenylmethanes by a herringbone or C−H···π arrangement.[2b,3] So its absence in the present family of structures needs some explanation. It would appear that the V-shaped conformation is stabilized by several intermolecular C−H···O hydrogen bonds[18] (d, 2.53−2.74 Å) between the activated C−H groups (adjacent to the nitro group) and the nitro O-atoms. Each molecule of **1** is connected to four others from adjacent stacks by two distinct sets of centrosymmetric C−H···O hydrogen bonds. These patterns are only possible with the V-shaped conformation and are shown as synthons **I** and **II** (Figure 2). The phenyl rings involved in this mode of association form a ring over bond overlap optimizing the local dipole−dipole/π···π

(12) Sheldrick, G. M. *SADABS*; Program for Empirical Absorption Correction of Area Detector Data; University of Göttingen: Göttingen, Germany, 1996.

(13) (a) Sheldrick, G. M. *SHELXS-97*; A Program for the Solution of Crystal Structures; University of Göttingen: Göttingen, Germany, 1997. (b) Sheldrick, G. M. *SHELXL-97*; Program for the Refinement of Crystal Structures; University of Göttingen: Göttingen, Germany, 1997. (c) Sheldrick, G. M. SHELXS-86. *Acta Crystallogr.* **1990**, *A46*, 467−473. (d) Sheldrick, G. M. *SHELXL-93*; A Program for the Refinement of Single-Crystal Diffraction Data; University of Göttingen: Göttingen, Germany, 1993.

(14) *Cerius^2 Program*; Molecular Simulations: 9685 Scranton Road, San Diego, CA 92121-3752, USA, and 240/250 The Quorum, Barnwell Road, Cambridge CB5 8RE, UK.

(15) Ahlrichs, R.; Bär, M.; Häser, M.; Horn, H.; Kölmel, C. *Chem. Phys. Lett.* **1989**, *162*, 165−169.

(16) Dewar, M. J. S.; Zoebisch, E. G.; Healey, E. F.; Stewart, J. J. P. *J. Am. Chem. Soc*. **1985**, *107*, 3902−3909.

(17) Allen, F. H. *Acta Crystallogr.* **1998**, *A54*, 758−771.

(18) Desiraju, G. R.; Steiner, T. *The Weak Hydrogen Bond in Structural Chemistry and Biology*; Oxford University Press: Oxford, 1999.

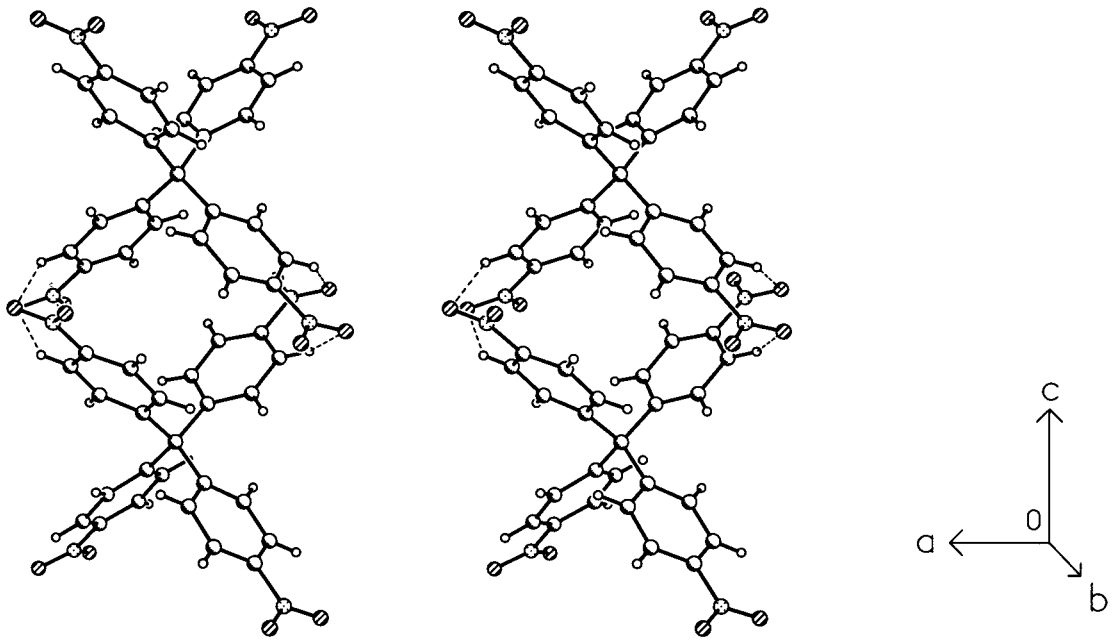

Figure 1. Stereoview of phenyl embrace in **2**. Notice the weak C−H···O hydrogen bonds. All such interactions in this and subsequent figures are indicated as broken lines.

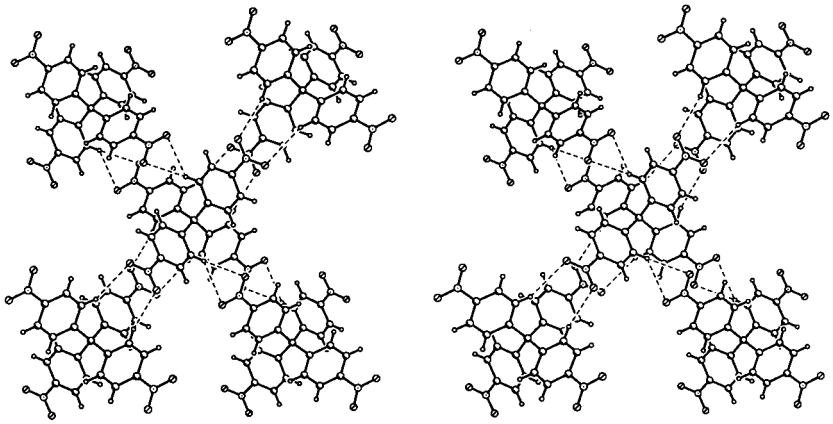

Figure 2. Four-fold connectivity of host molecules in **2** mediated by synthons **I** and **II**. The arrangement is nearly tetrahedral.

interactions. The nitrobenzene dimer energy in solvate **2** is −1.37 kcal/mol compared to −4.00 kcal/mol for the completely

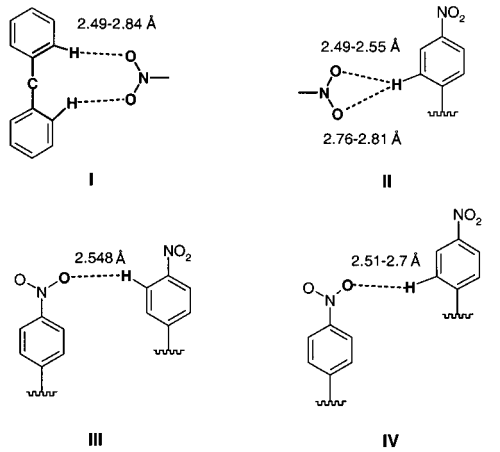

optimized dimer. So while there is some stabilization in **2**, it is not optimal, indicating that the demands of the dipole−dipole interactions, *ortho ortho* H-atom repulsions and C−H···O hydrogen bonding, are in conflict.[19] The result is a sandwich arrangement of aromatic residues that constitutes the spacer unit in a diamondoid network structure.[20]

The diamondoid network in **2** is unprecedented in that it is made up of weak interactions only (C−H···O hydrogen bonding and $\pi\cdots\pi$ stacking). Two such independent networks interpenetrate in the normal mode[21,22]with the second network related to the first by a 2-fold axis parallel to [100] and therefore separated by a half translation along [001] (Figure 3a). The interaction between the two independent networks is therefore the embrace stacking shown in Figure 2, with a separation of

(19) In fact the subtle variation or relationship between synthons **I** and **II** can be seen in Figure 2. A slight movement of the nitroaromatic group will generate synthon **II** from synthon **I** with a small decrease in the dipole−dipole/$\pi\cdots\pi$ interaction energy. Minor variations in both synthons can generate a number of intermediate possibilities without any significant loss in energy.

(20) Cozzi, F.; Cinquini, M.; Annunziata, R.; Dwyer, T.; Siegel, J. S. *J. Am. Chem. Soc.* **1992**, *114*, 5729−5733.

(21) According to Batten and Robson, there are two types of interpenetration, namely, normal and abnormal. In normal *n*-fold interpenetration, a translation along the direction of the shared 2-fold axis of 1/*n* times the length of the adamantanoid unit corresponds to one of the unit cell dimensions (generally the shortest). In abnormal interpenetration, the nets are not related by the usual translation of 1/*n* of the distance across an adamantane unit but by other symmetry elements. The only known example of the latter situation is the 5-fold interpenetration seen in adamantane-1,3,5,7-tetracarboxylic acid.[5e]

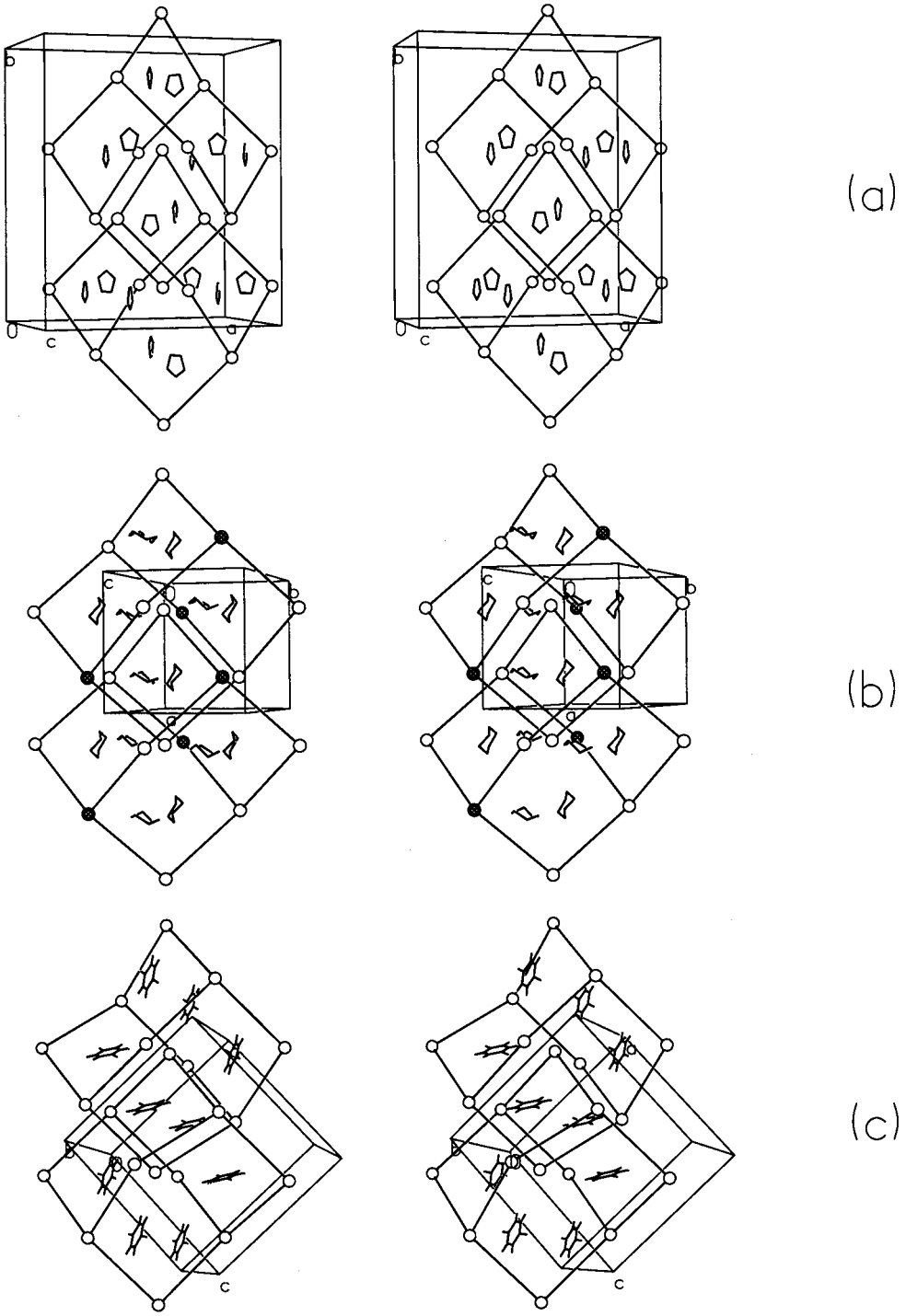

Figure 3. From top to bottom, parts a−c: Stereoviews along the channel direction in solvates **2**, **3**, and **5**. Host molecules **1** are reduced to spheres. In part b, the two different host molecules in the asymmetric unit are denoted by different shading. Notice the varying guest densities along the channel direction.

7.694 Å. As is well-known, such an interpenetrated diamondoid arrangement leads to the formation of channels along [001].[6b] In these channels are located the THF molecules, which are bisected by the 2-fold axes parallel to [010] (Figure 3a). The guest molecules in the channels are further stabilized by C−H···O hydrogen bonds. To summarize then, the structure of the THF solvate of compound **1** is a 2-fold interpenetrated diamondoid network with the connectors being a double layer of C−H···O and $\pi\cdots\pi$ linked aromatic residues, and with the solvent lying in the channels that are formed along the direction of interpenetration.

(b) Solvates 3 and 4, $(1)_3\cdot(\text{dioxane})_2$ and $(1)_3\cdot(C_6H_5NO_2)_2$. These 2-fold interpenetrated structures are very similar to the THF solvate, **2**. There are slight differences based upon the higher crystal symmetry (space group $P4_2/n$) and the presence of two symmetry-independent molecules of the host. These are present in a 2:1 ratio and are located on $\bar{4}$ and 2 axes. In Figure

(22) The degree of interpenetration is what would be predicted from the length-to-radius ratio of the spacer. The length and radius ratio of the rods that connect the tetrahedral centers have an influence on whether interpenetrative growth occurs. In general, it is expected that the larger this ratio, the more likely would be the interpenetration.[7c] In **2**, the ratio of length to radius is ∼3.5.

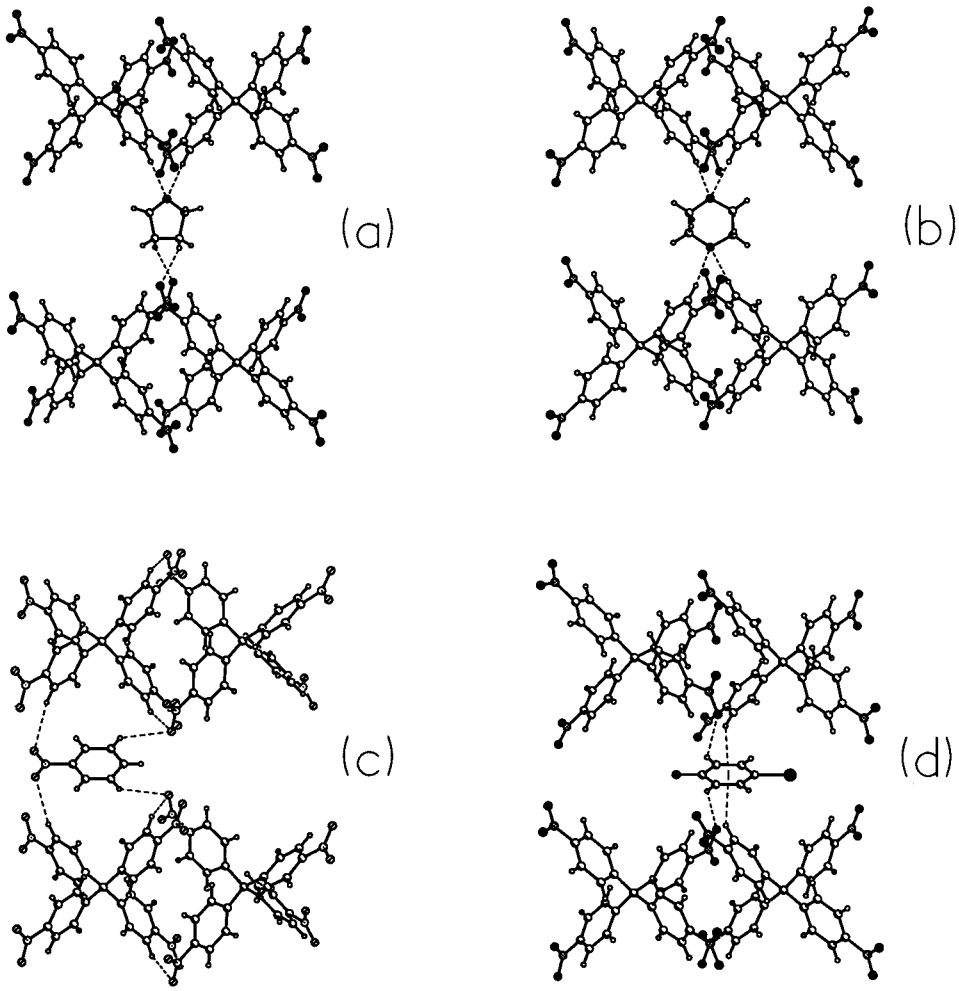

Figure 4. Parts a−d: Host···guest interactions in solvates **2**, **3**, **4**, and **5**, respectively, viewed perpendicular to the channel direction. Notice the symmetrical interactions of dioxane with the host structure in **3**. Also notice similar orientations of aromatic guests in **4** and **5** at different positions along the channel. The C−H···π interaction predominates in **5**.

3b they are shown respectively as shaded and open circles. Channels are formed along [001] and the guest molecules lie on 2-fold axes parallel to [001]. The guest molecules are stabilized via C−H···O hydrogen bonds to the host framework. Since two symmetry-independent host molecules are present, there are two molecule−molecule repeat or phenyl embrace, distances (7.831 and 7.854 Å) corresponding to white−white and white−black separations in Figure 3b. The smaller solvent stoichiometry when compared to solvate **2** may be ascribed to the slightly larger size of the dioxane and nitrobenzene molecules relative to THF.[23]

(c) Solvates 5−9, (1)$_2$·(solvent). The guest species in the isostructural solvates **5**−**9** are respectively 4-bromoanisole, anisole, phenetole, *p*-xylene, and chlorobenzene. Compound **1** is freely soluble in these aromatic solvents and so they were chosen for recrystallization. The similarity of these structures to those of solvates **2**−**4** is seen by an inspection of Figure 3 and Table 1. The minor variations, in terms of synthons **I** and **II** and other intermediate structures,[19] are mostly due to changes in crystal symmetry (space group *Pbcn*) and can be assumed as being a consequence of the guest molecule structure. The molecule−molecule repeat distances (phenyl embrace) are in the range 7.83−7.86 Å. Host−guest interactions include not only C−H···O hydrogen bonds but also C−H···π interactions to the aromatic solvents as acceptors. The solvent molecules are disordered in keeping with their location on various symmetry elements in the crystal even as the aromatic ring retains a similar orientation in all the cases. In **5**, the 2-fold axis bisects the molecule and the Br and OMe are positionally disordered. In **6**, there is 2-fold disorder of the OMe group. In **7**, the ethoxy group is similarly disordered. In **8**, the guest molecule is bisected by the 2-fold axis and so the Me group is rotationally disordered. The disorder in the chlorobenzene solvate **9** is similar to that in 4-bromoanisole **5**.

Broadly speaking, structures **2** through **9** may be described as doubly interpenetrated diamondoid networks of host molecules **1**, with the channels thus generated being occupied by the respective guest molecules (Figure 4). The host structure, mediated by synthons **I** and **II**, is virtually identical in all these cases. The host−guest stoichiometry varies, however, with the size of the guest. For the smallest guest, THF (volume 79 Å^3), this stoichiometry is 1:1. For dioxane (88 Å^3) and nitrobenzene (108 Å^3) it is 3:2, and for the larger benzenoid guests (volume range 99−129 Å^3) it is 2:1. While there is some evidence for host···guest interactions of the C−H···O and C−H···π type, the graded variations in host−guest stoichiometry (and perhaps their easy tendency to exhibit disorder) suggest that it is mostly

(23) Considering that the stoichiometry of the solvate seems to be determined by guest volume, it is a matter for further discussion if the crystal symmetry depends on the stoichiometry. In the present case, a host−guest 3:2 stoichiometry is nicely adjusted with the presence of two symmetry-independent host molecules present in a 2:1 ratio, and this in turn leads conveniently to tetragonal symmetry.

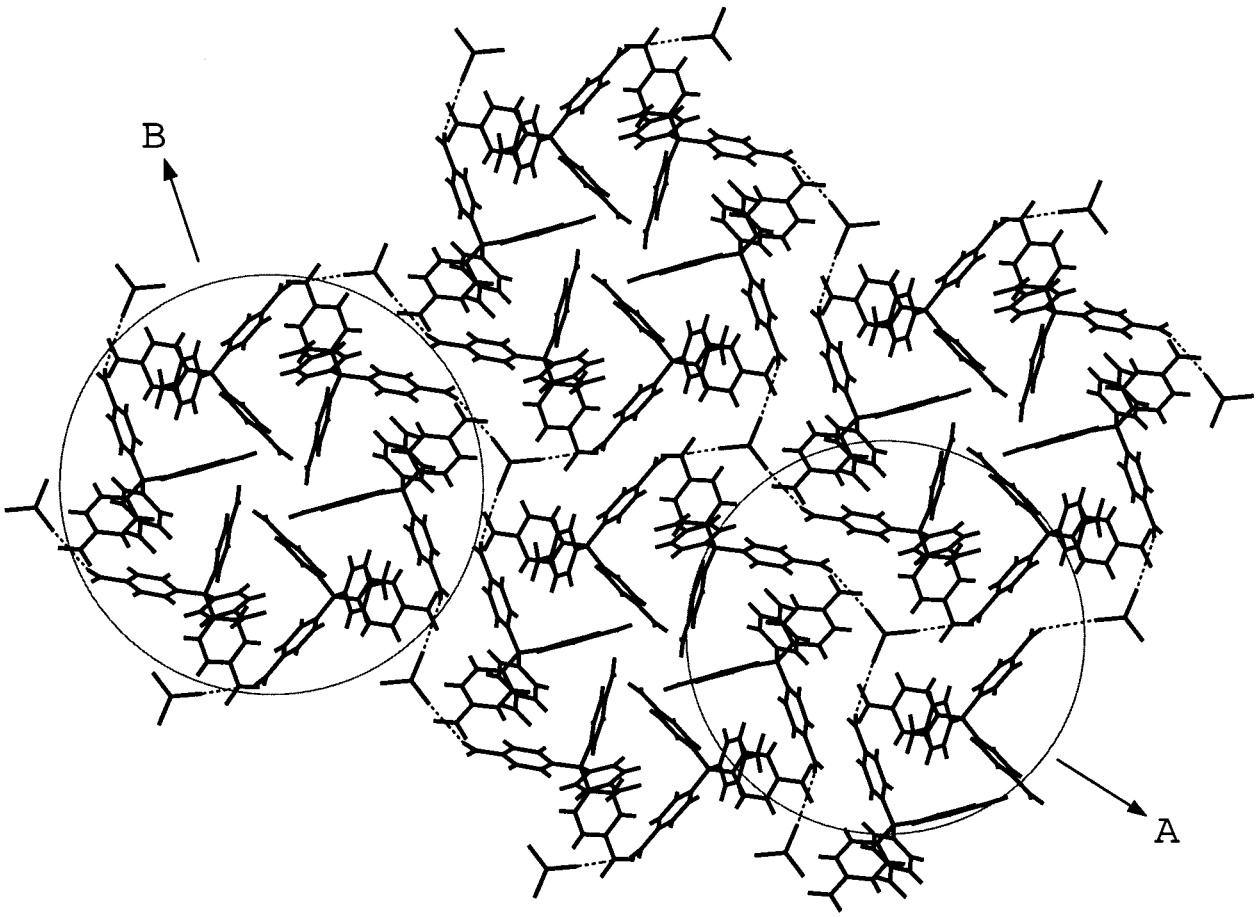

Figure 5. Hexagonal arrangement of components in solvate **10**. The two motifs A and B are indicated (see text).

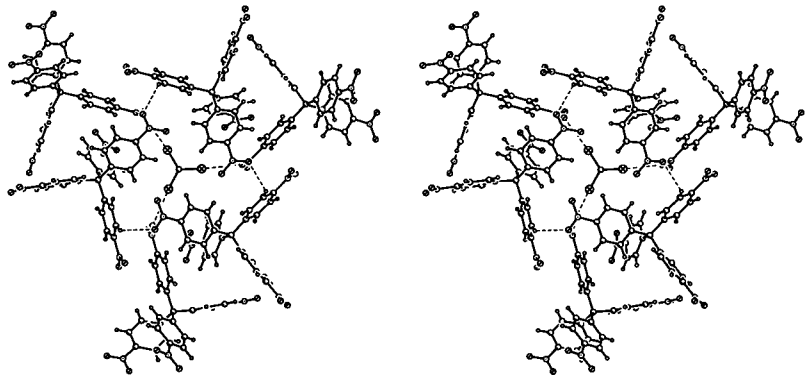

Figure 6. Motif A in solvate **10**. Notice that the $CHCl_3$ is connected to three molecules of **1** via $Cl\cdots O_2N$ interactions. The three other host molecules are connected to each other with synthon **III**.

close-packing that dictates the arrangement of guest molecules in the host channels.[24] As corroborative evidence, it was noted that there is a greater or lesser tendency for loss of solvent from all these solvates. To summarize, structures **2** through **9** resemble each other closely and are referred to hereafter as the diamondoid group.

Rhombohedral Group. (a) Solvates 10, 11, and 12, $(1)_3\cdot(CHCl_3)$, $(1)_3\cdot(CHBr_3)$ and $(1)_3\cdot$(DMF). These layered, rhombohedral structures (space group $R\bar{3}$) are strikingly different from those in the diamondoid group. Figure 5 shows the layer structure that may be further dissected into trigonal motifs A and B. The entire structure is based on a strong and distinctive pattern of interactions around the guest molecule. Indeed, so rigidly are the guests held by the surrounding host molecules that they are not lost upon heating right up to the respective decomposition temperatures, which are more than 100 °C above the boiling points of the guests. Let us consider the chloroform solvate, **10**, first. In motif A (Figure 6), each solvent molecule is positioned on a 3-axis and interacts with three host molecules via $Cl\cdots O_2N$ interactions (3.09 Å). There is adequate precedent for this type of interaction.[25] The three other host molecules in the figure dovetail such that a phenyl ring is placed in the

(24) It is not fully clear why nitrobenzene forms a solvate with 3:2 host−guest stoichiometry unlike the other aromatic solvents which give a 2:1 stoichiometry. For instance both chlorobenzene with a smaller volume (99 $Å^3$) and anisole with a larger volume (111 $Å^3$) give a 2:1 stoichiometry. However, the interaction pattern with nitrobenzene is slightly different in that $C-H\cdots\pi$ interactions are (not unexpectedly) absent.

(25) Allen, F. H.; Lommerse, J. P. M.; Hoy, V. J.; Howard, J. A. K.; Desiraju, G. R. *Acta Crystallogr.* **1997**, *B53*, 1006−1016. Desiraju, G. R.; Pedireddi, V. R.; Sarma, J. A. R. P.; Zacharias, D. E. *Acta Chim. Hung.* **1993**, *130*, 451−465.

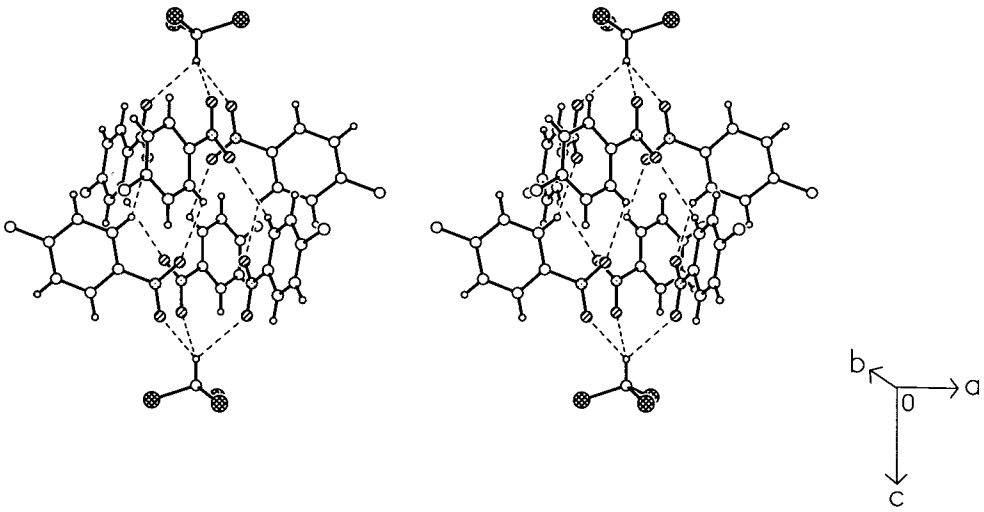

Figure 7. Central portion of Motif B in solvate **10**. Host molecules are connected with synthon **I**. Notice the trifurcated C−H···O hydrogen bonds from two $CHCl_3$ molecules. The other three nitrophenyl substituents on the central C-atom are not shown for clarity.

V-shaped cleft of the neighbor. To our knowledge, this kind of phenyl embrace (3-fold embrace) has not been documented so far. In motif B, there are two solvent molecules whose C−H groups point toward each other (Figure 7). The C−H groups act as trifurcated donors to nitro O-atoms (*d*, 2.468 Å; *θ*, 129°), and there is much precedent and evidence for chloroform to participate in such C−H···O hydrogen bond formation.[26] The B motif is completed by a ribbon of C−H···O bonds involving the *meta* C−H groups of the phenyl rings and the O-atoms of the nitro groups that do not form hydrogen bonds with chloroform.[27] Each particular $CHCl_3$ molecule is hexa-coordinated and may be associated with an A motif (where it is attached by three Cl···O interactions) and the adjacent B motif (where it acts as a trifurcated hydrogen bond donor). The entire arrangement may therefore be abbreviated as ...ABA ABA ABA... along the 3-axis.

The bromoform solvate, **11**, is isostructural to the chloroform solvate, **10**. The Cl···O_2N interactions in motif A are replaced by Br···O_2N that are actually slightly shorter (3.08 Å). This is characteristic of a halogen interaction that is polarization induced.[28] The C−H···O interactions are very similar to those in **10**. While the structural identity between the chloroform and bromoform solvates is hardly surprising, what is unique is that DMF also forms a rhombohedral structure, **12**, with a packing that is very similar to the other two. The DMF molecule is disordered with its N and O atoms lying on the 3-axis. The two methyl groups and the formyl C−H group are disordered between three sites and there are differences in interaction environment between the haloform guests and DMF. Instead of the Cl/Br···O_2N and Cl_3CH···O interactions, there are three sets of C−H···O interactions involving the methyl groups as donors, the carbonyl oxygen as a trifurcated acceptor, and the formyl C−H group as a possible donor.[18] The entire arrangement is without precedent, and to our knowledge, there is no prior example of DMF acting as a trigonal mimic via such disorder. As in the case of the haloform solvates, it is impossible to remove DMF from solvate **12** without completely decomposing the crystal.

Three Distinct Solvent-Rich Structures. (a) Mesitylene Solvate 13, (1)·(C_9H_{12})$_2$. There are two symmetry-independent guest molecules. Each host molecule is networked to four others: to two via synthon **I** as in the diamondoid group and to two others somewhat formally via C−H···O bonds (2.57 Å, 175°). Three of these connections (including the two that use synthon **I**) are shown in Figure 8 from which it will be seen that a large hexagonal shaped cavity is created wherein are located a pair of guest molecules, corresponding to one of the symmetry sites. Figure 9 shows the network structure of the host and the profusion of guests in this structure (two different symmetry sites are indicated by light and bold lines). The guest molecules shown in Figure 8 form a stacked dimer (3.61 Å) of the inversion type (light molecules in Figure 9) while the other symmetry-independent guest molecules (dark in Figure 9) lie nearly along the phenyl embrace direction and are aligned almost parallel to one of the nitro aromatic rings (3.40 Å), indicating the importance of $\pi\cdots\pi$/donor−acceptor interactions. The two symmetry-related inverse dimer guest molecules also form such $\pi\cdots\pi$/donor−acceptor interactions (3.64 Å) with nitrobenzene rings from two different **1** molecules (Figure 8). As might have been expected, solvent is lost rapidly from this solvate, leading to microcrystalline material.

(b) Collidine Solvate 14, (1)·($C_8H_{11}N$). Crystallization of **1** from 2,4,6-trimethylpyridine was attempted to establish isostructurality with the mesitylene solvate, **12**. However, the result turned out to be quite different. Each host molecule is networked to eight others via the single interaction synthon **III**, in a manner reminiscent of body-centered cubic packing (Figure 10). The collidine guest is situated in the octahedral site of the BCC lattice and disordered in a unique manner over four sites related to one another by $\bar{4}$ symmetry. The disordered guest molecules are stabilized in the host cavity by very weak $\pi\cdots\pi$/donor−acceptor interactions supported presumably by dipole−dipole interactions (3.84 Å). This elongated distance may be a reflection of the weak donor capability of collidine compared to mesitylene (HOMO:LUMO energies are −9.1602:0.5716 and −9.3568:0.2371 eV for mesitylene and collidine, respectively).

(c) *o*-Xylene Solvate 15, (1)·(C_8H_{10})$_2$. It is well-known from the field of coordination polymers that 4-connected nets may be either tetrahedral or square.[29] Solvate **15** is a good example of a square net (Figure 11). The molecules are connected with synthon **IV**. Symmetry-independent guest molecules are located

(26) Glasstone, S. *Trans. Faraday Soc*. **1937**, 200−214.

(27) It is also possible that there are specific nitro···nitro interactions in the B motifs according to the model suggested previously, see: Wozniak, K. *Polish J. Chem.* **1997**, *71*, 779−791.

(28) Desiraju, G. R.; Harlow, R. L. *J. Am. Chem. Soc*. **1989**, *111*, 6757−6764

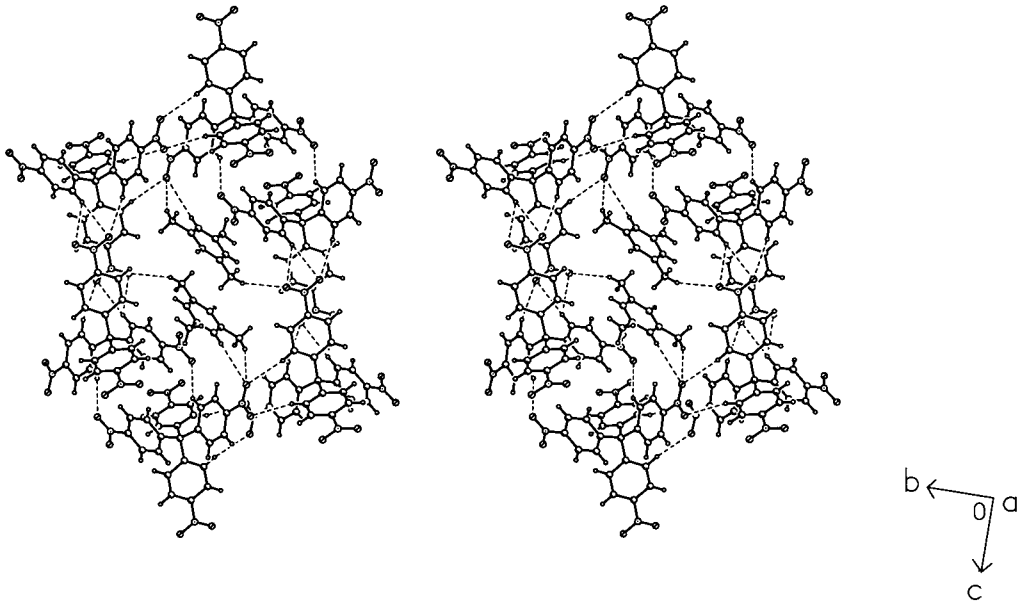

Figure 8. One of the two symmetry independent mesitylene guests in **13** in the open host framework

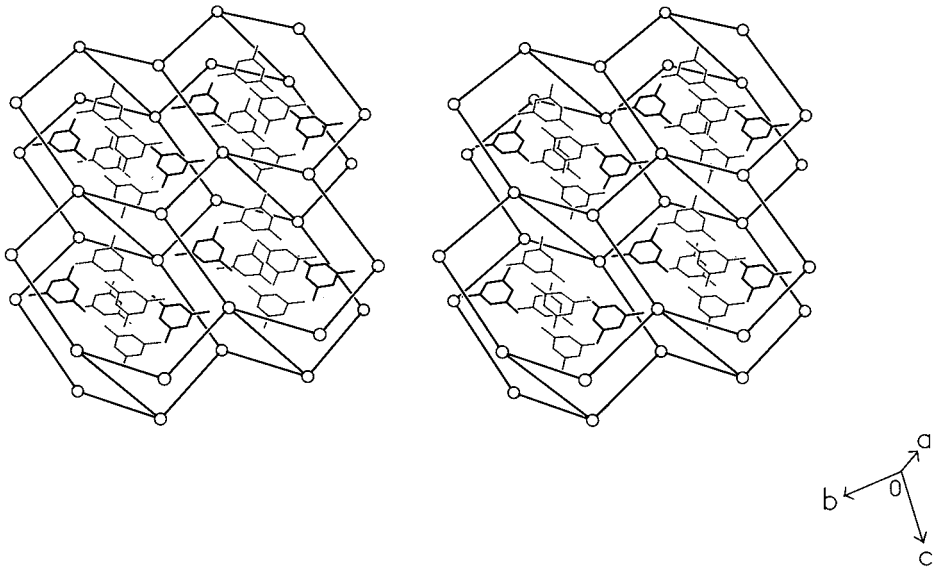

Figure 9. Mesitylene molecules in the host framework of solvate **13**. Stacked dimers (represented by thinner lines) occupy the bigger windows that run along [100] while other symmetry-independent guest molecules (thicker lines) run along smaller windows nearly parallel to [010].

in alternating squares. Adjacent nets related by 2-symmetry are also shown in the figure from which it may be noted that the solvent lies in channels. Unsurprisingly, solvent loss from **15** is facile. A large number of C−H···O interactions in the range 3.51 to 3.70 Å between and within host and guest are observed. Again, and as in the diamondoid group, it was noted that the host network is constituted only with weak hydrogen bonds, which is a novel aspect of this study.

Analysis and Correlation of the Structures of Solvates 2 through 15. A distinctive feature of the structures described above is the wide differences between the diamondoid group, the rhombohedral group, and the three individual solvent-rich structures. Also noteworthy are the more subtle variations within the diamondoid group. All this suggests that the structures obtained follow from the solvent used for crystallization—in other words **2** through **15** are all examples of guest-induced host assembly. This dependence of overall structure on the nature of the guest has to do with not only the particular packing and interactions involved but also the guest−host stoichiometry.

The various structural groups may be considered with respect to synthon **I**. In the diamondoid group (Figure 2) each molecule of **1** is connected symmetrically to four others with synthon **I**. Both C−H···O hydrogen bonds and dipole−dipole interactions are optimized in the process. In the rhombohedral group too, synthon **I** is found. This is shown explicitly in Figure 12. However, only two of the four near neighbors are connected with synthon **I** with the two others linked via single-point interactions. In the mesitylene solvate **13** there are three synthon **I** linkages (the fourth forming a donor−acceptor stacking interaction between guest and host). It would appear that **I** is the dominant mode of association of host molecules with deviations caused by specific intermolecular interactions (rhom-

(29) (a) Holý, P.; Závada, J.; Císarová, I.; Podlaha, J. *Angew. Chem., Int. Ed.* **1999**, *38*, 381−383. (b) Sharma, C. V. K.; Rogers, R. D. *Cryst. Eng.* **1998**, *1*, 19−38. (c) Davies, C.; Langler, R. F.; Sharma, C. V. K.; Zaworotko, M. J. *Chem. Commun.* **1997**, 567−568. (d) Brunet, P.; Simard, M.; Wuest, J. D. *J. Am. Chem. Soc.* **1997**, *119*, 2737−2738. (e) Glidewell, C.; Ferguson, G. *Acta Crystallogr*. **1996**, *C52*, 2528−2530. (f) Subramanian, S.; Zaworotko, M. J. *Angew. Chem., Int. Ed. Engl*. **1995**, *34*, 2127−2129.

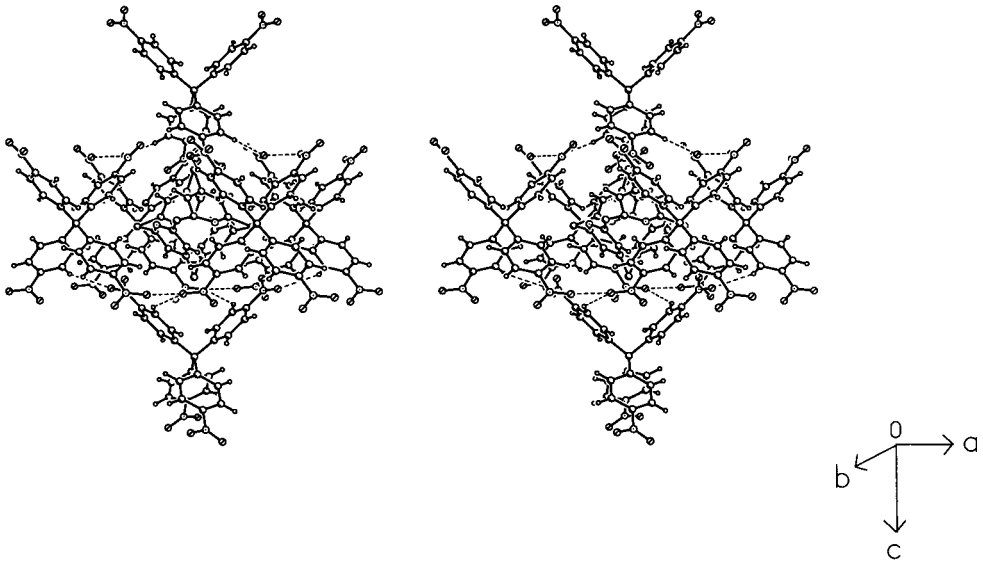

Figure 10. Eight-fold coordination of host molecules in solvate **14**. Notice synthon **III**.

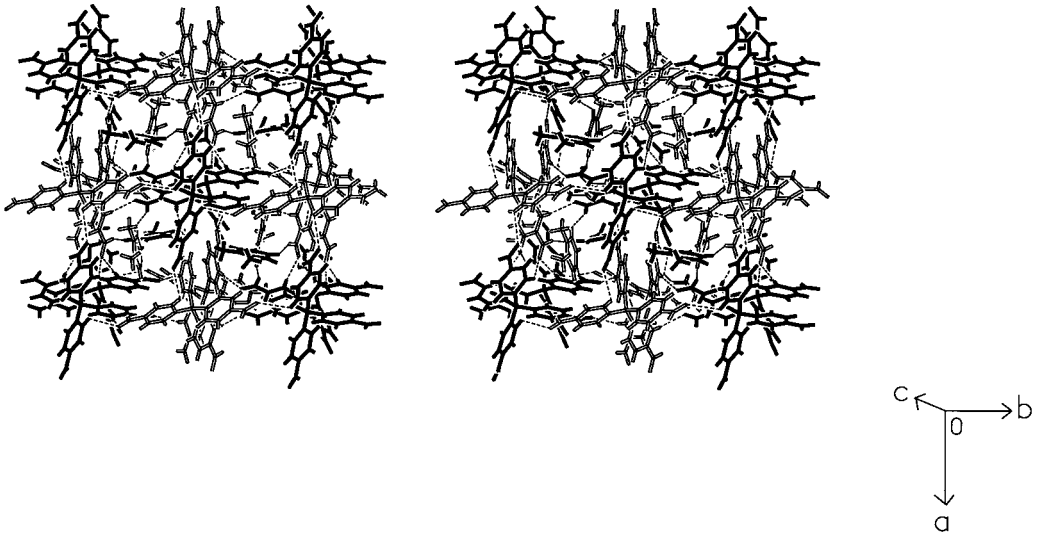

Figure 11. Square network arrangement of host molecules connected by synthon **IV** in solvate **15**. View down [001]. Different shading is used for symmetry-independent molecules. The guest *o*-xylene is also shown.

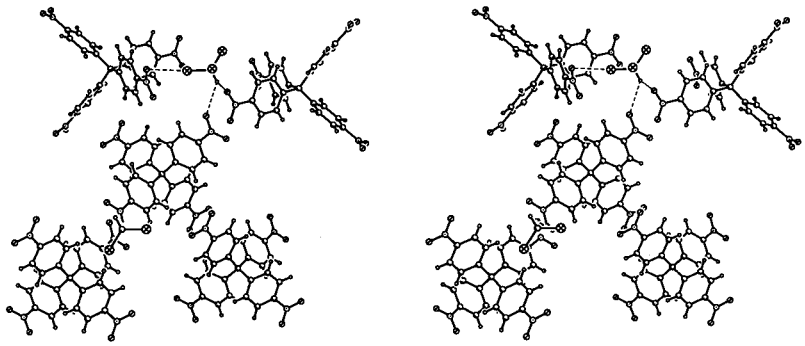

Figure 12. Host molecules in chloroform solvate **12** showing host···host coordination. Compare with Figure 2.

bohedral group) or the need to include more solvent (mesitylene).

As to why mesitylene does not form a solvate in the diamondoid group, it is instructive to examine Figure 13, which shows the diamondoid structures down the $\bar{4}$ direction. The shapes of the channels are interestingly different. The channel in the dioxane solvate is more circular and matches the symmetrical C−H···O interactions on both sides of the guest molecule which straddles the channel (Figures 3 and 4). The channels in the THF solvate (Figure 13b) and the anisole subgroup (Figure 13c) are more elliptical and the solvents are now situated length downward (Figures 3). The molecular width in the anisole subgroup is probably just enough to match the molecular dimensions of **1** and its propensity to form synthon **I**. Mesitylene is, in this sense, too large a molecule to fit into such channels and, lacking the capability to form specific host−

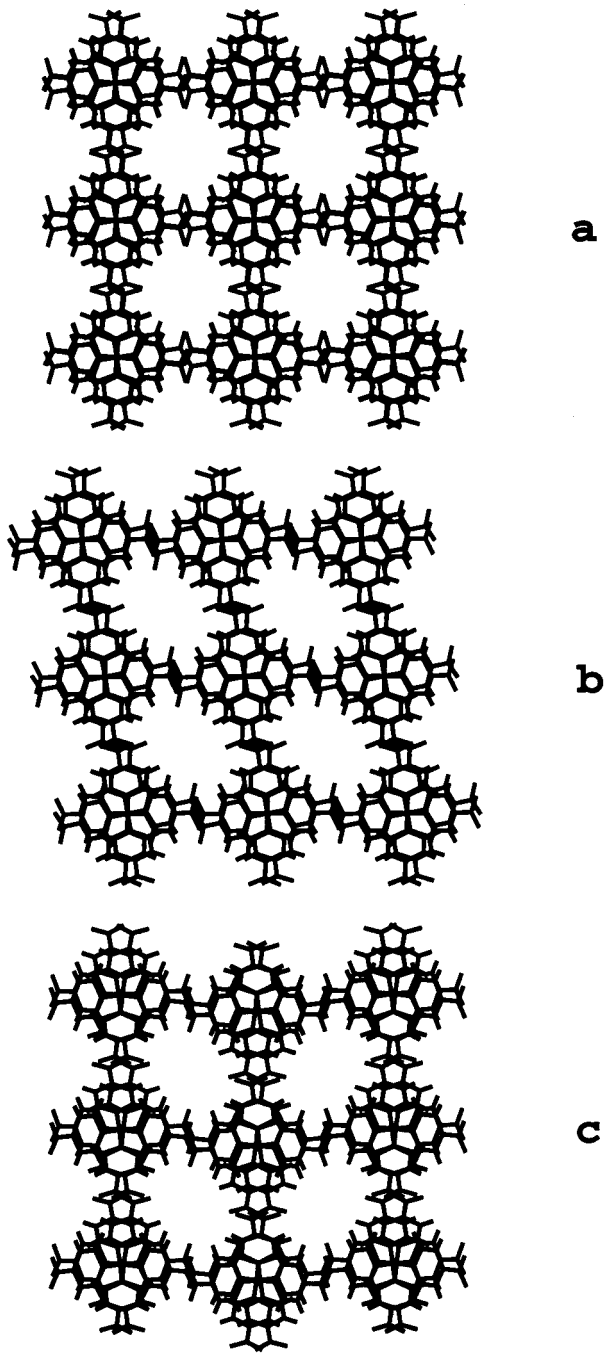

Figure 13. A view down the channel axis of structures in the diamondoid family. Guest molecules are removed for clarity. (a) Symmetrical channel in **3** and **4**. (b) Ellipsoidal channel in **2**. (c) Ellipsoidal channel in the *Pbcn* structures of **5**−**9**. Notice the slight differences in the channel cross-sections and alignment.

guest interactions characteristic of the rhombohedral group, it adopts a more open solvent-rich variation, **13**. One might have expected collidine with a size and shape very similar to mesitylene to form a similar solvate. The very different structure of solvate **14** suggests that chemical factors are important. The reduced donor capability of collidine relative to mesitylene is revealed in the long $\pi\cdots\pi$ separation (3.84 Å) in **14** relative to **13** (3.40 and 3.64 Å). Indeed, it might be suggested that the very unusual disorder of the collidine guest in the host cavity results from the absence of specific guest−host interactions, both species containing electron-poor aromatic rings.

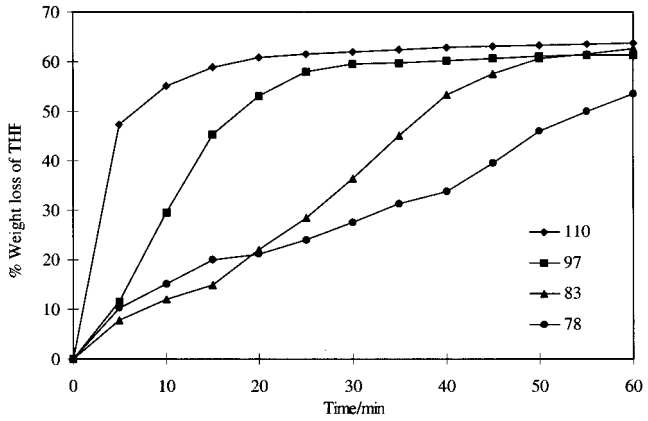

Figure 14. Desolvation of solvate **2** at elevated temperatures.

The decisive role that specific chemical interactions play in determining crystal structures is seen in the solvent-poor rhombohedral group. The diamondoid structure is not an option for the haloform guests because they cannot fit into the channels formed in that structure. The high host to guest stoichiometry in solvates **10** through **12** hints that specific chemical factors are important in the rhombohedral packing, but mere stoichiometry cannot be taken as proof of the fact. Rather, it is the pronounced tendency of the haloforms to participate in $X\cdots O_2N$ and $X_3C-H\cdots O$ interactions that would appear to favor the high-symmetry packing actually observed. The molecules of **1** make good use of 3-fold symmetry for both the interaction types referred to above, and the interactions themselves are considerably shorter than the respective van der Waals separations. Indeed, these solvates may be termed molecular complexes rather than inclusion compounds, even as it is realized that the difference between such terms can be subjective in the limit.

The orientation of the DMF molecule in solvate **12** is further evidence of the importance of specific directional interactions in this group of structures. That DMF would form a solvate in the rhombohedral group was not really anticipated but given that it does, it would be reasonable to assume that the 3-fold disordered $(CH_3)_2NCHO$ acts as a shape and size mimic to X_3CH because of the chloromethyl exchange rule.[30] However, the sense of the haloform molecules and DMF along the 3-fold axis is the opposite, and this is due to the very specific interactions formed by these guest molecules. The haloforms are involved in $X\cdots O_2N$ interactions along the $+c$ sense and this is matched by the $X_3C-H\cdots O$ interactions along $-c$. The DMF on the contrary donates $C-H\cdots O$ hydrogen bonds along $-c$ and accepts them along $+c$, giving rise to an opposite orientation relative to the haloforms. Packing energy calculations and packing coefficients (Table 2) reveal nearly similar host−host interactions in solvates **2**−**12** while in solvent-rich **13**−**15** these are far less, being compensated by host−guest and to some extent guest−guest interactions.

In summary, the three groups of structures studied here—rhombohedral (**10**−**12**), diamondoid (**2**−**9**), and miscellaneous (**13**−**15**)—span a range of host-to-guest stoichiometries. The diamondoid and miscellaneous groups may be regarded as being characterized by comparable host···host and host···guest interactions while in the rhombohedral family the host···guest interactions dominate. The rhombohedral group represents the

(30) (a) Muthuraman, M.; Fur, Y. L.; Bagieu-Beucher, M.; Masse, R.; Nicoud, J.-F.; George, S.; Nangia, A.; Desiraju, G. R. *J. Solid State Chem.* **1999**, *152*, 221−228. (b) Desiraju, G. R.; Sarma, J. A. R. P. *Proc. Indian Acad. Sci. (Chem. Sci.)* **1986**, *96*, 599−605.

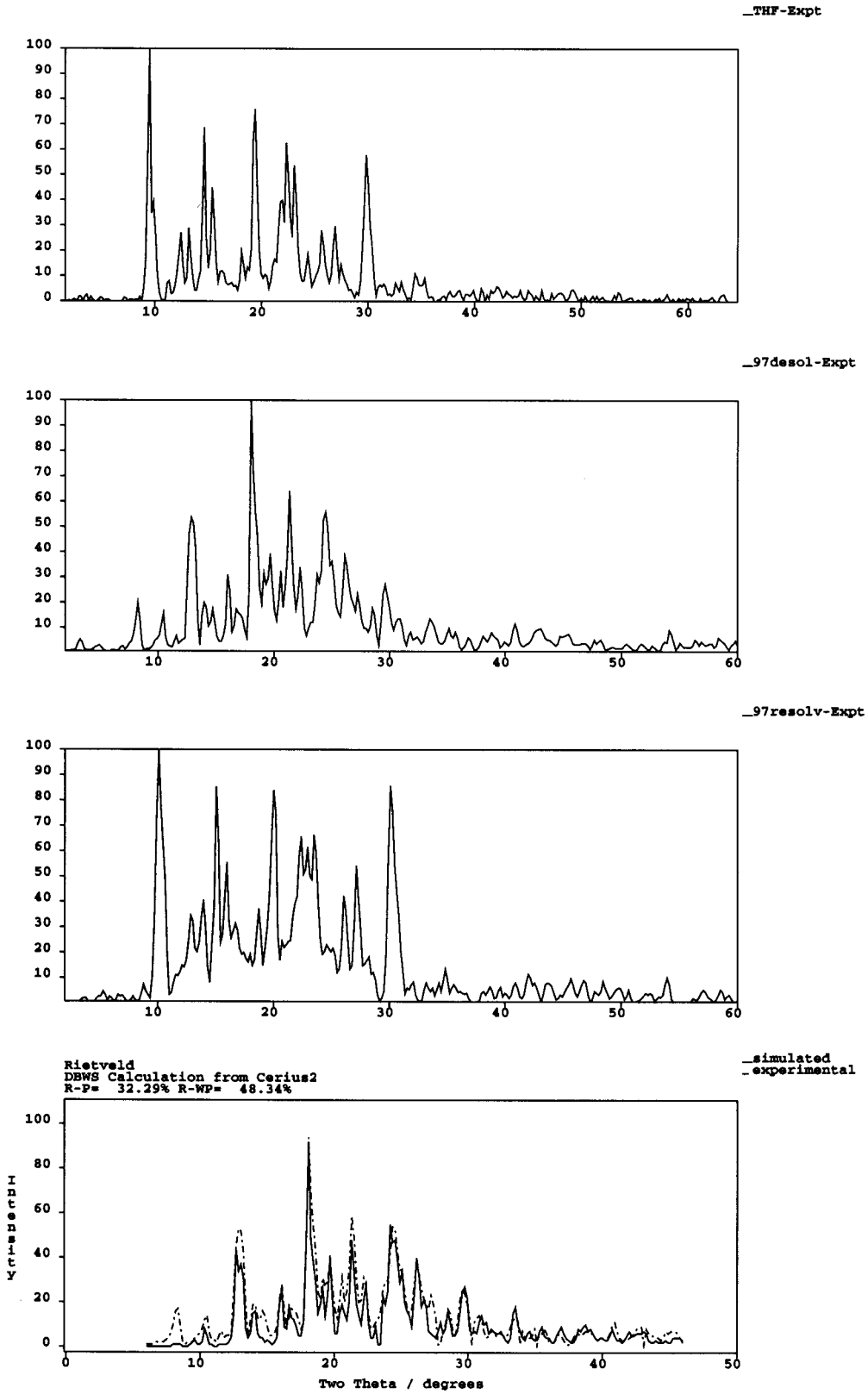

Figure 15. X-ray powder spectra of solvate **2**: (a) the powder spectrum of initially recrystallized material; (b) desolvated material (at 97 °C for 2 h); (c) resolvated material (compare with part a); and (d) simulated spectrum (solid line) using Rietveld refinement compared with part b represented by dashed lines.

solvent-poor domain and consists of structures from which it is not possible to remove solvent by heating, short of decomposing the material. The diamondoid group samples the solvent-rich domain. Here, solvent may be removed to varying degrees as will be seen in the following section. Structures in the miscellaneous group are very rich in solvent and do not retain it at all unless precautions are taken. All these solvates have been obtained by recrystallization from excess solvent at room temperature. The particular structure formed depends on the solvent chosen.

Structural Transformations. (a) Loss of THF from Solvate 2. Crystalline **2** was heated at 65, 78, 83, 97, and 110 °C for 2

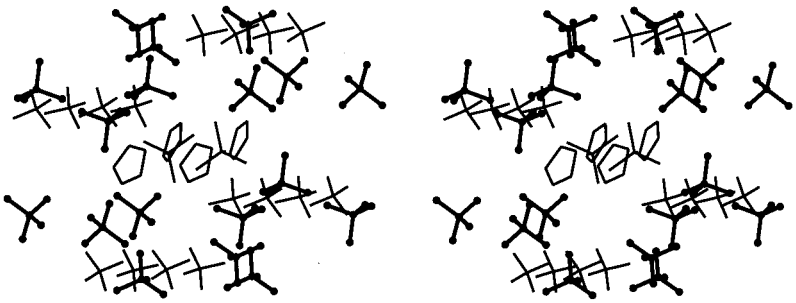

Figure 16. Overlay diagram of solvates **2** and **10** along the channel axis. The molecules of the host **1** are represented as tetrahedra for clarity. Thinner tetrahedra indicate host molecules in solvate **2**, while thicker tetrahedra represent those in the chloroform solvate **10**.

h under a mild vacuum. The guest loss is minimal, about 12% when the sample was heated at 65 °C for 2 h. At higher temperatures (78 °C and above), the weight loss is continuous for about 2 h and until it tapers off at 62−65%. These details are plotted in Figure 14. More drastic conditions (110 °C, 24 h) do not cause more solvent to be lost. Some representative X-ray powder diffraction traces for these samples are given in Figure 15. The powder trace for the sample heated at 65 °C is indistinguishable from that of the original solvate **2**. The traces for the samples heated at 78, 83, 97, and 110 °C are very similar, but are now completely different from the original pattern. Analysis of these traces revealed that the peak profiles are similar to those of the rhombohedral group with the maximum intensity at a *d* spacing of 4.9 Å corresponding to the (3 1 2) planes. We infer that the material undergoes a transformation from THF-*Fddd* (THF-I) with a 1:1 stoichiometry to THF-$R\bar{3}$ (THF-II) with a 3:1 stoichiometry. This latter stoichiometry is in accordance with the nearly 65% solvent loss.

Further evidence for the structure of the rhombohedral THF-II form was obtained by its fortuitous appearance, when **1** was crystallized from a 1:1 mixture of THF and chlorobenzene.[31] Solution ^{1}H NMR showed the presence of THF in the crystals but not of chlorobenzene. X-ray single-crystal diffraction analysis of the THF-II showed the packing of molecules of **1** to be identical with that of the rhombohedral group, **10**−**12**; however, the guest THF is highly disordered on the 3-fold axis.[32] Only three C-atoms of the guest molecule could be located from the electron density map. However, the simulated powder spectrum of this rhombohedral form matches almost exactly the powder trace of the sample of **2** heated at 110 °C for 1 h. More satisfyingly, it was found that the reversible THF-I → THF-II → THF-I cycle of transformations could be carried out on the same sample. When single crystals of THF-I were heated at 97 °C for 2 h, the material became opaque. When this resulting THF-II form was wetted in a minimum amount of THF for a month at 0 °C, the material became translucent (not completely transparent).[33] It was possible to collect single-crystal diffraction data on this heated and soaked crystal. The cell dimensions so obtained correspond to the THF-I form.[34] These transformations are illustrated via X-ray powder diffractograms in Figure 15. From Table 2, it may be noticed that the rhombohedral group is associated with high packing energies and packing coefficients. The rhombohedral structure is therefore the thermodynamically more stable one.

The mechanism of transformation of THF-I to THF-II may be understood from the relationship between the rhombohedral and diamondoid structures. In Figure 16, the THF solvate **2** and the chloroform solvate **10** are plotted on the same figure and down the channel direction. For simplification, the host molecules are abbreviated to tetrahedra: light for solvate **2** and dark for **10**. The guest molecules are shown in full. Some of the host molecule positions are practically unchanged in the two structures. Molecules in these sites do not move in the transformation. As the guest molecules from the THF-I form escape upon heating and the crystal lattice generally loosens, some of the host molecules are able to slide and reorient themselves around the channel axis increasing the coordination number from four to six around the solvent axis.[35,36] The reader can easily identify the slipped molecules: these are the ones where the positions of the light and dark tetrahedra in the figure do not overlap. Yet, with each light tetrahedron (molecule of host in THF-I) may be associated a dark tetrahedron (molecule of host in THF-II), thereby mapping out pathways for molecules to reorient themselves.

(b) Solvation of the Rhombohedral THF-II Form. To further examine the conditions under which reversible transformations between the two THF forms occur, samples of solvate **2**, heated at 83, 97, and 110 °C for 2 h, were soaked in a minimum amount of THF at 0 °C for 10 days. The powder spectra of the 83 and 97 °C samples showed almost complete resolvation to the THF-I form (Figure 15). However, the powder pattern of the 110 °C sample was unchanged after soaking in THF and solvation back to THF-I did not occur. Clearly, the orthorhombic to rhombohedral transformations are reversible only at and below some temperature between 97 and 110 °C. It would appear that when the solvent loss exceeds a critical amount (close to 65%), the structure gets irreversibly locked into the rhombohedral form. The rhombohedral form is capable of transformation back to the diamondoid form at solvent losses below this critical region. The diamondoid form is completely porous to external solvents. When single crystals and powders

(31) Reasons for the formation of this THF-II from mixed solvent remain speculative at best.

(32) Crystal data for the THF-II measured on Enraf Nonius MACH 3: host:guest ratio, 3:1; space group, $R\bar{3}$; rhombohedral cell parameters: a = 15.351(2) Å, α = 92.08(2)°; R = 0.051, $wR2$ = 0.1227 for 4230 data and 356 parameters; goodness-of-fit index = S = 1.069.

(33) These conditions were worked out so that no part of the material dissolved in the solvent, as far as could be made out by visual inspection.

(34) Cell parameters for the THF-I obtained by soaking THF-II in solvent: a = 14.31(1) Å, b = 14.33(1) Å, c = 16.197(7) Å, α = 104.22(4)°, β = 104.70(6)°, γ = 115.85(5)°, which may be transformed into the *Fddd* unit cell with a = 15.21 Å, b = 24.27 Å, c = 28.59 Å, which are comparable with those of **2** (Table 1).

(35) Simultaneously there is change between the 4-fold phenyl embrace of the diamondoid group to the 3-fold phenyl embrace of the rhombohedral group

(36) Such transformation is seen in the topological rearrangement within a single crystal from a honeycomb $Cd(CN)_2$ three-dimensional net to a diamondoid net when the crystal of $Cd(CN)_2$ obtained from 50% aqueous *tert*-butanol was exposed to chloroform vapors, see: Abrahams, B. F.; Hardie, M. J.; Hoskins, B. F.; Robson, R.; Williams, G. A. *J. Am. Chem. Soc.* **1992**, *114*, 10641−10643. For a very recent example of excellent guest exchange in a coordination polymer, see: Noro, S.; Kitagawa, S.; Kondo, M.; Seki, K. *Angew. Chem., Int. Ed.* **2000**, *39*, 2082−2084.

of solvate **2** were soaked in solvents such as dioxane, 4-bromoanisole, *o*-, *p*-, and *m*-xylenes, mesitylene, and collidine, most of the THF was replaced by dioxane, 4-bromoanisole, and *p*-xylene. Mesitylene, collidine, and *o*- and *m*-xylene were not so effective in displacing the THF in the channels. These observations are in accord with shape and size considerations.

Conclusions

A number of conclusions may be drawn from this work: (1) Compound **1** is a new host material, whose versatile guest-inclusion properties have been discovered by chance rather than by design.[37] Notwithstanding the numerous efforts that have attempted to rationally design new host materials, it is an indisputable fact that a large number of these have been discovered accidentally. Perhaps this is an indication as to how little we really know about crystal packing in a general sense. (2) Solvates **2** through **9** in this study constitute the first example of a robust diamondoid network built with weak interactions, in this case C−H···O and $\pi\cdots\pi$ hydrogen bonds. In the present context, robustness of a host framework refers to its stability with respect to guest removal and guest exchange. (3) The solvates studied here are a very good example of a pseudopolymorphic system. Indeed it was impossible to isolate guest-free host material. Pseudopolymorphs are solvated forms of a compound, which have different crystal structures and/or differ in the nature of the included solvent. The former criterion is exemplified by considering, say, the THF and the chloroform solvate, the latter by considering the THF and dioxane solvate. In general, and to simplify matters, all the solvates **2** through **15** may be called pseudopolymorphs.[38] (4) Finally, the solvates of compound **1** present a system where modulation between two distinct structure types is possible. This modulation occurs by removal or introduction of solvent. Each structure type, diamondoid or rhombohedral, retains its integrity over certain conditions, is capable of reversible transformation to the other under specific conditions, and in the high-temperature, solvent-poor limit transforms irreversibly into the rhombohedral form. This is unusual behavior in host−guest chemistry; generally a host network is robust and withstands any kind of removal or introduction of guest molecules, or is so fragile that it collapses completely upon removal of guest. Here, we have an example where the host network is in part robust and in part flexible. Perhaps one could attribute this fluxional nature of the host network to the weakness of the connecting interactions. If so, this represents a new dimension to the study of weak hydrogen bonds, one in which their weakness may be exploited to obtain structural flexibility and dynamics.

Acknowledgment. This work is supported by grant 01-(1570)/99/EMR-II of the Council of Scientific and Industrial Research, Government of India and Hong Kong Research Grants Council Earmarked Grant CUHK 4206/99P. We thank Dr. Ashwini Nangia and Dr. D. Shekhar Reddy for discussions. R.T. acknowledges the University Grants Commission, New Delhi for the award of a fellowship. G.R.D. thanks Molecular Simulations Inc. (Cambridge) for their continuing support and cooperation.

Supporting Information Available: Additional figures and hydrogen bond geometries, tables of crystal data, structure solution and refinement, atomic coordinates, bond lengths and angles, and anisotropic thermal parameters for **2**−**15** (PDF). This material is available free of charge via the Internet at http://pubs.acs.org.

JA0031826

(37) Bishop, R. *Synlett* **1999**, 1351−1358.

(38) (a) Sarma, J. A. R. P.; Desiraju, G. R. *Crystal Engineering*; Seddon, K. R., Zaworotko, M., Eds.; Kluwer Academic Publishers: Dordrecht, The Netherlands, 1999; pp 325−356. (b) Kumar, V. S. S.; Kuduva, S. S.; Desiraju, G. R. *J. Chem. Soc., Perkin Trans. 2* **1999**, 1069−1073. (c) Nangia, A.; Desiraju, G. R. *Chem. Commun.* **1999**, 605−606.